



Published in final edited form as:

*Chem Biol.* 2008 December 22; 15(12): 1317–1327. doi:10.1016/j.chembiol.2008.10.014.

## The Importance of Odorant Conformation to the Binding and Activation of a Representative Olfactory Receptor

Zita Peterlin<sup>1,3</sup>, Yadi Li<sup>2,3</sup>, Guangxing Sun<sup>2</sup>, Rohan Shah<sup>2</sup>, Stuart Firestein<sup>1</sup>, and Kevin Ryan<sup>2,\*</sup>

<sup>1</sup>Department of Biological Sciences, Columbia University, New York, NY 10027, USA

<sup>2</sup>Department of Chemistry and Biochemistry, City College of New York, and Graduate School, City University of New York, New York, NY 10032, USA

### SUMMARY

Olfactory receptors (ORs) form a large family of G-protein coupled receptor proteins (GPCRs) responsible for sensing the ambient chemical environment. The molecular recognition strategies used by ORs to detect and distinguish odorant molecules are unclear. Here, we investigated the variable of odorant carbon chain conformation for an established odorant-OR pair: n-octanal and rat OR-I7. A series of conformationally restricted octanal mimics were tested on live olfactory sensory neurons (OSNs). Our results support a model in which unactivated OR-I7 binds aliphatic aldehydes indiscriminately, and then applies conformational and length filters to distinguish agonists from antagonists. Specific conformers are proposed to activate OR-I7 by steric buttressing of an OR activation pocket. Probing endogenously expressed rat OSNs with octanal and constrained mimics furnished evidence that odorant conformation contributes to an odorant's unique olfactory code signature.

### INTRODUCTION

The sense of smell begins with molecular recognition of a chemical odorant by one or more olfactory receptors (ORs) expressed in the olfactory sensory neurons (OSNs) of the nasal epithelium (Firestein, 2001; Reed, 2004; Touhara, 2002). The ORs are members of the G-protein coupled receptor (GPCR) family of membrane-bound proteins (Buck and Axel, 1991). OR activation by an odorant agonist initiates the transduction of chemical structure information into a neural activity code that ultimately gives rise to the perception of an odor. An odorant may also bind an OR without triggering signal transduction, contributing to the olfactory code by competitively antagonizing a receptor's activation by other odorant agonists present in a mixture (Araneda et al., 2000; Araneda et al., 2004; Oka et al., 2004). The rodent and human genomes encode over 1000 ORs, though in humans many of these are pseudogenes (Niimura and Nei, 2007). The combinatorial use of the set of ORs enables an individual to detect and distinguish far more airborne chemicals than there are individual ORs (Malnic et al., 1999; Oka et al., 2004).

\*Correspondence: kr107@sci.ccnycuny.edu Ph. (212) 650-8132; Fax (212) 650-6107.

<sup>3</sup>These authors contributed equally to this work.

**Publisher's Disclaimer:** This is a PDF file of an unedited manuscript that has been accepted for publication. As a service to our customers we are providing this early version of the manuscript. The manuscript will undergo copyediting, typesetting, and review of the resulting proof before it is published in its final citable form. Please note that during the production process errors may be discovered which could affect the content, and all legal disclaimers that apply to the journal pertain.

Olfactory GPCRs have had to evolve to recognize small molecules that disperse into the air. Hence, odorants are typically low molecular weight and uncharged. Many odorants are hydrocarbons or very hydrophobic molecules containing a single heteroatom, most often oxygen. Many olfactory GPCRs must consequently bind odorants without the benefit of multiple polar interactions common to other small molecule-protein associations such as enzyme-substrate associations, or those pertaining to the aminergic GPCRs (Shi and Javitch, 2002). Like rhodopsin and other Class A GPCR family members, ORs are predicted to have 7 transmembrane (TM)  $\alpha$ -helices and to bind their ligands in a site bounded by TMs 3, 5, 6 and possibly 4 and 7 (Abaffy et al., 2007; Hall et al., 2004; Katada et al., 2005; Pilpel and Lancet, 1999; Singer, 2000). ORs exhibit a high degree of sequence variability within these helices as expected for a family of proteins that binds diverse ligands. In the hypervariable TM regions where contact with odorants is predicted to occur, there is a strong bias toward hydrophobic aliphatic and aromatic residues, a weaker bias towards polar uncharged residues, and a bias against charged residues (Pilpel and Lancet, 1999). Difficulties obtaining atomic level structural information on transmembrane proteins have prevented a detailed understanding of the strategies used by olfactory GPCRs to discriminate their odorant ligands.

It has long been known that a single OSN can be activated by a range of related odorants (Firestein et al., 1993; Ma and Shepherd, 2000; Sato et al., 1994; Sicard and Holley, 1984). Evidence continues to accrue in support of the idea that each OSN expresses only one of its ~1000 genomic ORs (Chess et al., 1994; Malnic et al., 1999; Serizawa et al., 2004). It follows that each OR must be able to recognize multiple odorants. This has been demonstrated experimentally, though the structural relatedness of the activating odorants varies from receptor to receptor (Araneda et al., 2000; Kaluza and Breer, 2000; Krautwurst et al., 1998; Malnic et al., 1999; Raming et al., 1993; Touhara et al., 1999; Zhao et al., 1998). Perhaps to ensure surveillance of as much chemical space (Dobson, 2004) as possible, the receptive ranges of ORs overlap, with a single odorant typically activating multiple ORs. Different odorants, even those that are structurally related, appear to activate unique subsets of ORs, ultimately giving rise to a unique olfactory experience and forming the basis of the olfactory code (Malnic et al., 1999).

To understand the olfactory code at the chemical level will require a precise understanding of the chemical determinants responsible for activating and blocking each OR. Several studies have cited molecular "length" as one such determinant (Araneda et al., 2000; Ho et al., 2006; Kaluza and Breer, 2000; Malnic et al., 1999; Mori et al., 1999). Length studies have focused mainly on odorants containing aliphatic carbon chains (Araneda et al., 2000; Ho et al., 2006; Kaluza and Breer, 2000; Malnic et al., 1999). These studies used homologous series of conformationally flexible n-alkyl acids, aldehydes, ketones and alcohols. However, the conformational flexibility of such odorants leaves unclear the true molecular length required for activation because aliphatic odorants exist in large ensembles of conformational isomers. This uncertainty also raises the question whether ORs bind odorants in preferred conformations - such as an extended conformation, as implied in the previous studies - but disfavor the same odorants when presented in other conformations. Moreover, GPCR binding and GPCR activation may have different conformational requirements. To address the variable of odorant conformation as a factor in the molecular receptive range of a representative OR, we have assayed a series of conformationally restricted analogs of octanal, the primary agonist for the rat I7 olfactory receptor (OR-I7). Testing these new compounds has provided insight into the activation and blocking of the OR-I7 receptor, and has demonstrated how conformational flexibility influences the total number of ORs activated by a single odorant.

## RESULTS

The rat OR-I7 receptor is one of the few ORs to have been cloned, expressed in neurons and functionally characterized by probing with a large collection of odorants (Araneda et al., 2000; Araneda et al., 2004; Krautwurst et al., 1998; Zhao et al., 1998). OR-I7 is activated by multiple aliphatic aldehydes having a length between  $\sim 8\text{\AA}$  and  $\sim 12\text{\AA}$  (Araneda et al., 2000). We note that multiple conformations are possible for aliphatic aldehydes. We therefore define length here to mean the length of the longest attainable (and typically lowest energy) conformation (see Experimental Procedures). The most potent OR-I7 ligand found thus far is octanal, referred to hereafter as **C8** (for 8 carbon n-alkanal; likewise for **C7**, **C6** etc.). Like many ORs, OR-I7 is activated by odorants with successive carbon chain lengths centered on the most potent ligand (Kaluza and Breer, 2000; Malnic et al., 1999). In the rat nasal epithelium, **C8** activates more cells and elicits a greater cAMP (the signal transduction second messenger) response than do shorter and longer homologs (Kaluza and Breer, 2000), indicating that the dimensions of the OR-I7 binding site are likely close to average. OR-I7 is thus typical and well characterized, ideal for a systematic investigation of the effect of odorant conformation on its receptive range.

### A series of conformationally restricted eight-carbon aldehydes

**C8** is highly flexible, having six rotatable bonds that can each adopt three different conformations: one anti, or one of two gauche. The maximum number of formally possible conformational isomers is  $3^6 = 729$ , though symmetry makes some equivalent and undoubtedly reduces this number. Nothing is known about the bound conformation of **C8**. On the one hand, were **C8** to bind and activate OR-I7 in one or a small subset of favored conformers, it would incur a conformational entropy penalty in the free energy of binding due to the loss of conformational flexibility. In this case, preorganizing **C8** to resemble the bound conformation should improve binding by minimizing the loss of entropy. On the other hand, a previous study compared the calculated lowest energy conformation of a group of activating ligands and concluded that OR-I7 may tolerate a number of structural variations at the carbons most distant from the aldehyde (Araneda et al., 2000), possibly indicating that many different **C8** conformers are capable of activating OR-I7. To gain insight into the activating conformation(s) of **C8**, we made a series of eight-carbon aldehydes with restricted conformations (Fig. 1A). Conceptually, carbon eight (denoted as  $C_8$ ) of **C8** was tied back by establishing a new bond successively to  $C_7$  through  $C_2$ , yielding compounds **1-6**, respectively. Unlike the previously studied series of homologous n-alkanals, in which the partition coefficient and other physical properties can vary with the number of carbons in the chain, we expect to maintain throughout our eight-carbon series similar physical-chemical properties while reducing the number of possible conformations. This strategy should enable us to study effects that occur at the level of the OR binding pocket while minimizing receptor-independent effects. In this series the maximum length of the aldehydes is also progressively shortened. Due to the conformational restriction, the maximum length is now a better estimation of this dimension compared with the n-alkanal series. The synthesis of these analogs was straightforward and is summarized in Fig. 1B.

### OR-I7 activation: Octanal uses a semi-extended conformation

The new eight-carbon aldehydes were tested via calcium imaging of dissociated rat neurons expressing recombinant OR-I7 from an adenoviral vector as previously described (Araneda et al., 2004). As an example, the activation of OR-I7 by analog **3** is shown in Fig. 2A. Responses were concentration dependant and saturating. At high concentrations, the magnitude of the response to analogs **1**, **2** and **3** saturated with efficacies comparable to that of **C8**; no partial agonists were detected. Analog **4**, **5** and **6** failed to reach saturation over this concentration range. Activation curves for the entire series, including **C8**, are shown in Fig. 2B, which also

tabulates the concentrations at which half maximal activation is reached ( $EC_{50}$ ). The new compounds segregate into two groups. Compounds **1**, **2** and **3**, which have smaller rings and four to six freely rotatable bonds, all strongly activated OR-I7, while compounds **4**, **5** and **6**, which contain larger rings and one to three rotatable bonds, activated OR-I7 weakly or not at all. The greatest difference in activity, 163-fold, was observed between compound **4** (6.3Å,  $EC_{50} = 748 \mu\text{M}$ ) and compound **3** (7.0Å,  $EC_{50} = 4.6 \mu\text{M}$ ). The n-alkanals of five to twelve carbons (**C5** to **C12**) were previously tested against OR-I7 in the vapor phase using electroolfactogram (EOG) recordings (Araneda et al., 2000; Zhao et al., 1998). By that method, the largest difference in activity in the series fell similarly between **C6**, (no activation, 6.4Å) and **C7**, (activation, 7.6Å). Thus, using the new series of **C8** analogs, we confirmed that there is a minimum length requirement for activation, and further narrow it down from 6.4Å–7.6Å to 6.5Å–6.9Å. We interpret the finding that an aldehyde of only 7.0Å is sufficient to activate the receptor, compared to the extended length of **C8** (8.9Å), to mean that **C8** does not activate OR-I7 in its fully extended conformation, but rather adopts one or more semi-extended conformations to do so. The poor activity in the eight carbon aldehydes **4–6**, where the variables of total carbon number and length are separated, defines the shorter end of the activating length cut-off, and provides evidence that **C8** does not activate OR-I7 while in compact conformations approximating those mimicked by **4–6**.

### Small cycloalkyl rings enhance OR-I7 activation

To test whether maximum length is solely responsible for the difference in activity observed among compounds **1–6**, we obtained the full activation curves for **C7** and **C6** by calcium imaging (Fig. 3). Although **C7** and compound **2** have identical extended lengths, **2** was 40-fold more potent (Fig. 3A). Compound **2** was even more potent than **C8**.

Similar to previous OR-I7 EOG recordings (Araneda et al., 2000), calcium imaging revealed a sharp increase in activity (145-fold) in the step from **C6** to **C7** (Fig. 3B). The maximum length of compound **3**, which contains the cyclobutyl group, falls between those of **C7** and **C6** (Fig. 3C). Based on a correlation with maximum length, the activity of **3** should also fall between that of **C7** and **C6**. However, **3** was more potent than both (Fig. 3B), providing a second example where a small cycloalkyl ring increased potency beyond what was expected based on length alone. Thus, while the activity of the cyclic compounds generally required a certain minimum length, restricting the rotation of the terminal two or three bonds enhanced potency, indicating that specific conformations or shapes at the end opposite the aldehyde are preferred by the activating form of OR-I7.

### An activating octanal conformation

We next explored conformational restriction of **C8** towards the middle of the chain. In examining the data shown in Fig. 2B, we noted that all of the active compounds had a rotatable bond between  $C_4$ - $C_5$ , while in all inactive compounds this bond was locked in a ring. Although this observation might merely reflect the variable of length, in another study the same bond in *trans*-2-*cis*-6-nonadienal, an OR-I7 activating compound, was implicated as a potential pivot-point important for activation (Araneda et al., 2000). In the extended conformation, all of **C8**'s C-C bonds adopt the anti conformation (Fig. 4A, left). Rotation of the  $C_4$ - $C_5$  bond by  $120^\circ$  into a gauche conformation (Fig 4A, middle) reduces the total length of **C8** from 8.9Å to 8.0Å, provided the other bonds remain in the anti conformation. Changes of this nature could serve to reduce the actual length of the molecule into the type of semi-extended conformation proposed above. To test the effect of this particular alteration, we installed a two-carbon bridge from  $C_3$  of **C8** to  $C_6$  (Fig. 4A, right). The resulting six-member ring locked **C8** into a gauche conformation around  $C_4$ - $C_5$ . Imagining this process beginning with a rotation of the same bond in the opposite sense produces the same structure, due to symmetry. Compared to the 729 hypothetical conformations that **C8** can sample, the resulting **C8** analog, **11**, can exist in only

~10 closely related conformers. **11** was synthesized as a ~2.4:1 mix of the trans:cis isomers, as outlined in Fig. 4B and described in the Experimental Procedures.

Unable to separate these two isomers, we tested **11** as a mixture. In the case where one isomer is inactive - or perhaps even an antagonist - testing the mixture incurs the risk of underestimating the true response of the other isomer. Despite this concern and the introduction of a six-member ring into the middle of **C8**, the isomeric mixture of **11** was more active than **C8**, shifting the activation curve slightly to the left (Fig. 4C). Just as **C8** is two carbons longer than the much less potent **C6**, compound **11** is two carbons longer than the nearly inactive **5**, and the gain in activity might appear to correlate merely with the increase in extended conformation length (the cis isomer of **11** is ~7.4Å and the trans is ~8.0Å). However, in contrast to **C8**, the two terminal carbons of **11** are fixed by the ring in their relation to the aldehyde group, though in slightly different locations in the two isomers. If we assume that the orientation of the aldehyde group with OR-I7 is fixed in the odorant binding site, then the three dimensional coordinates of the ethyl group of **11** must likewise be fixed and occupy a distal (to the aldehyde) activating region in the receptor. **11** may therefore resemble an, or the, activating conformation of **C8**, just as **4**, **5** and **6** are constrained to resemble inactive conformations.

### Conformational determinants of OR-I7 antagonism

In nature, odorants are typically encountered in mixtures. In this context, each odorant can activate one set of receptors while simultaneously antagonizing a subset of receptors activated by other components, leading to great complexity in the olfactory code at the level of sensory input (Araneda et al., 2000; Araneda et al., 2004; Malnic et al., 1999; Oka et al., 2004). Most OR antagonists discovered to date are structurally related to the agonists whose activity they suppress (Araneda et al., 2000; Araneda et al., 2004; Oka et al., 2004). Interestingly, natural product fragrances typically contain structurally related odorants (Arctander, 1960), suggesting a potential evolutionary significance.

We thus set out to systematically probe the length and conformation requirements for antagonism of OR-I7 by simultaneously applying a saturating concentration of **C8** (10 μM) and increasing concentrations of either the inactive **C8** analogs **5** and **6**, or the similarly inactive **C4** and **C5**. The marginally active **C6** and **4** were also used. Unexpectedly, nearly all were capable of antagonizing **C8** activation, suggesting a broad antagonist receptive field with regard to the hydrophobic portion of short aldehydes. A representative calcium imaging trace is shown in Fig. 5A. Here, analog **6**, which itself cannot activate OR-I7, is shown to antagonize **C8** activity. Inhibition curves for **4**, **5**, **6**, **C4**, **C5** and **C6** are shown in Fig. 5B with the concentration of each required for 50% inhibition (IC<sub>50</sub>) tabulated in Fig. 5C. Among the n-aldehydes, antagonist potency increased with the number of carbons in the chain. The failure of **C4** (3.9Å) to antagonize **C8** activation may indicate a minimum n-aldehyde chain length requirement for antagonism between 4.0Å and 5.1Å, but we cannot rule out receptor-independent effects, such as reduced hydrophobicity and increased water solubility due to the small size. Among the cycloalkyl ring containing aldehydes, where the constant number of carbons should control for receptor-independent effects, all were moderate antagonists but without apparent length dependence (Fig. 5C). In fact, the IC<sub>50</sub>s for the cyclic compounds were remarkably similar and each was a more potent antagonist than its closest length-matched n-alkanal. This result may indicate a dependence of antagonism on odorant surface area or carbon number in combination with a maximum length below 6.5Å-6.9Å. Taken together with the activation data, aldehydes that resemble **C8** in a compact conformation appear to be able to bind OR-I7 in its unactivated state, blocking subsequent activation by **C8**, while those that can extend beyond 6.5Å-6.9Å appear able to bind and stabilize OR-I7 in its activated state. Held close to the aldehyde, the large cycloalkyl groups appeared to enhance antagonism, just as the small cycloalkyl rings, held distant, enhanced activation. Overall, these results provide an

example where a structural trait, namely maximum attainable length, is correlated in a systematic way with the transition from antagonism to agonism.

### Functional group determinants of OR-I7 antagonism

The strict requirement of an aldehyde group for activation of OR-I7 is well established (Araneda et al., 2000). The results described above prompted us to ask whether antagonism also requires the aldehyde group. As shown in Fig. 5D, replacement of the aldehyde function in **C6** with a variety of other functional groups resulted in loss of antagonism. In combination with the activation data, this result means that the aldehyde group is necessary but not sufficient for binding to OR-I7. The attributes of the carbon chain complete the requirements for binding, and determine whether binding leads to activation or antagonism.

### Conformational flexibility contributes to the activation range of an odorant

OR-I7 is not the only **C8** receptor in the rat genome; **C8** is estimated to activate between 55 and 70 of the 1227 predicted (Gibbs et al., 2004) functional rat ORs (Araneda et al., 2004). It has long been suspected that highly flexible odorants activate more ORs than do less flexible odorants (Amoore, 1970; Kaluza and Breer, 2000). However, this possibility has previously only been examined using a series of odorants that vary in carbon number and thus in multiple physical properties (Kaluza and Breer, 2000). Our series of conformationally restricted **C8** analogs provided the opportunity to examine this question in a controlled manner, using **C8** as a representative odorant.

We assayed 1190 viable rat OSNs with 30  $\mu$ M **C8** and (individually) analogs **1-6**. The cells were also probed with forskolin, an activator of the signal transduction cascade that bypasses the OR to provide an internal standard for normalization of the OSN response to each odorant. Fig. 6A represents the entire population of cells that responded to at least one compound, showing how each cell discriminated among the eight-carbon aldehydes. The activation traces of three representative cells are shown in Fig. 6B. Overall, 5.9 % of OSNs (70/1190) were activated to some extent by **C8**, in close agreement with the earlier study (Araneda et al., 2004). **C8** and the less constrained (more rotatable bonds) analogs **1**, **2** and **3** activated approximately twice as many cells as did the most constrained analogs, **5** and **6** (Fig 6C, filled circles; 5.6, 6.2, and 6.2% vs. 3.4 and 3.6%, respectively). These data support the idea that, in general, the greater the flexibility of an odorant, the greater the number of ORs it will activate, even when the odorant's functional groups and number of carbons are held constant.

With the exception of one cell (Fig. 6A, cell #53), all **C8**-sensitive cells also responded to at least one of the cyclic analogs, consistent with the idea that our analogs sample sub-regions of the conformational space occupied by the ensemble of **C8** conformers detected by OSNs. None of the cells activated by **C8** responded equally to all analogs, which we interpret as evidence that conformational preference is a general underlying feature among **C8**-responding ORs, and not unique to OR-I7. Of the 70 cells that responded to **C8**, 39 (56%) responded more strongly to a cyclic analog than to **C8**. This high percentage was unexpected since **C8** is the only natural product in the series. One explanation is that for these OSNs, the most strongly activating cyclic analog is preorganized into a region of **C8**'s conformational space that binds and stabilizes the activating form of the single ORs expressed in these cells, so that less conformational entropy is lost upon activation. The overall free energy of binding should become more favorable and lead to greater potency versus **C8**. For each OSN that preferred a cyclic analog to **C8**, we calculated the difference in the normalized response magnitudes between its best-tuned analog (i.e. the most highly activating analog) for the OSN, and that of **C8** (Fig. 6D). Organizing the data in this way revealed a clear trend in which the difference in activation grew as the analogs became more conformationally restricted (fewer rotatable bonds). The more conformationally restricted compounds **5** and **6** may be viewed as frozen in conformations that mimic relatively

high-energy, rarely populated conformations of **C8**. The difference in strength of activation shown in Fig. 6D should reflect both the preorganization inherent in the analog and the difficulty **C8** has in adopting the conformation preferred by these OSNs. Rings are common in natural product odorants. Ring-containing odorants may achieve some of their odorant qualities by simulating conformations rarely adopted by acyclic compounds that otherwise contain a similar number of carbons and the same functional groups.

## DISCUSSION

Rhodopsin, the most frequently studied GPCR, evolved to respond to photons, but its activation is in fact triggered by the isomerization of a covalently held ligand (Sakmar et al., 2002). We consider this isomerization to be analogous to a conformational change, though one that depends on light. From this perspective, rhodopsin can be considered to exemplify the importance of ligand conformation to GPCR activation. ORs, which like rhodopsin belong to the Class A GPCR subfamily, have evolved to report on the chemical space of airborne molecules. An important variable in chemical space is shape, which in molecules with rotatable bonds is determined by conformation. Flexible molecules constantly change conformation, but to respond to all possible odorant conformations would be a stringent demand to place on an OR, which needs to maintain a degree of tuning specificity to contribute to the olfactory code. It is reasonable then to expect that molecular conformation is an important determinant of the receptive range of ORs and that, like rhodopsin, ORs will be stabilized in their activated and unactivated states by specific but divergent odorant conformations. The prevalence of carbocyclic rings in distinctive fragrance molecules, such as the santalols and terpenoids, among many others, reinforces this expectation. However, the difficulty in obtaining structural information on membrane-bound proteins has made this expectation impossible to verify experimentally.

We chose OR-I7 to investigate the importance of conformation to OR activation because it can be expressed recombinantly in OSNs and because its primary ligand, **C8**, has many rotatable bonds that can be selectively restricted in synthetic analogs designed to address specific hypotheses. In the **C8** analogs presented here (Fig. 1A), we chose to begin by keeping the number of carbons constant. This choice enabled us to progressively restrict the rotatable bonds of **C8** and to systematically shorten its length while maintaining similar physical properties such as lipophilicity. Using this series, we confirmed that molecular length is important to activity when the number of carbons is held constant (summarized in Fig. 7A): aldehydes **1**, **2** and **3** activated OR-I7 but **5**, **6** and, for the most part, **4** were too short to activate it, even though competition experiments demonstrated that they bound OR-I7. A previous rat OR-I7 study using n-alkanals had noted that **C8**'s activity was greater than that of **C7**, and that **C6** was inactive (Araneda et al., 2000). We noted a similar trend here (Fig. 7A) using a different method that permitted greater control over the concentration of applied odorant. The finding here and elsewhere (Araneda et al., 2000) that **C7** (7.6Å) produces significant OR-I7 activity can be taken as evidence that **C8** need not adopt its longest possible - and lowest energy - conformer (8.9Å) in order to activate OR-I7. The potent activity of **C8** analogs **2** (7.6Å) and **3** (7.0Å) further support the idea that **C8** activates OR-I7 in a shorter-than-extended conformation. The inability of the eight-carbon aldehydes **5** (5.4Å), **6** (4.7Å) and, with the exception of very high concentrations, **4** (6.3Å), to activate OR-I7 indicates, however, that extreme deviations from the extended conformation are inconsistent with activation, though not binding. This finding appears to rule out the possibility that OR-I7 is activated by tightly bent **C8** conformers resembling those mimicked by **4-6**. OR-I7 appears therefore to be activated by **C8** in a conformation whose length falls in a window somewhere between its extremes.

The restricted **C8** analogs also revealed that odorant length is not the sole characteristic of the carbon chain that determines OR-I7 activity. Within the window of activating lengths, the

activity of compounds **2** and **3** was anomalously high when compared to the n-alkanal series. For example, **C7** and **2** have the same maximum length, yet **2** was 40-fold more potent. This anomaly indicates that the rotational restriction of the last two or three carbons of a sufficiently long aldehyde enhanced its ability to activate OR-I7. OR-I7-activating aldehydes were previously thought to be insensitive to structural variability in this region because the predicted lowest energy conformations of a group of activating ligands showed variability there but not in the proximal C<sub>1</sub>–C<sub>4</sub> region (Araneda et al., 2000). Our results using restricted eight-carbon aldehydes show that terminal cyclopropyl and cyclobutyl groups can be potent substructures for OR-I7 activation. We speculate that the terminal methyl group in **C8** and **C7** can rotate away from a distal activating hydrophobic binding pocket through rotation of the C<sub>5</sub>–C<sub>6</sub> or C<sub>6</sub>–C<sub>7</sub> bonds, whereas in **2**, the analogous bonds are fixed by the cyclopropyl ring, perhaps forcing a portion of the ring to persist in contact with the pocket. (**C6** apparently reaches this hypothetical binding pocket much less efficiently.) In this regard, the receptive range of OR-I7 appears to be fine-tuned through the application of length and conformational filters, since the receptor binds a wider range of aldehydes than can proceed to activation.

What, then, is the activating **C8** conformation of OR-I7, and how does it stabilize activation? Using our activation data and information from a previous study (Araneda et al., 2000) we focused on the conformation around the C<sub>4</sub>–C<sub>5</sub> bond. A 120° rotation of this bond from the more stable anti to the less stable gauche conformation shortens and kinks the chain slightly. When locked into this conformation, the resulting **C8** analog **11** was more active (as a cis/trans mixture) than **C8**, despite the extra steric bulk of the two-carbon bridge. The closer of these two bridging carbons resembles a 3-methyl group, which in the context of similar aliphatic aldehydes is well-tolerated by OR-I7 (Araneda et al., 2000). Unlike the acyclic aldehydes, the stereochemical relationship between the aldehyde and the last two carbons of **11** is fixed by the ring to a small number of conformations. Because activity was preserved we conclude that **11** resembles an activating conformation of **C8**. Separate testing of the cis and trans isomers, and the synthesis of other analogs restricted in this part of **11**, will tell us if it resembles the only activating conformer, or if OR-I7 tolerates some conformational heterogeneity here.

A comparison of **11** to compound **5** is also informative (Fig. 4C). **5** lacks the ethyl group of **11** but is otherwise identical. The addition of this ethyl group to **5** was sufficient to convert it from an antagonist into an agonist of greater potency than **C8**. The ethyl group is therefore responsible for activation, though not for binding, and must somehow stabilize an activated conformation of OR-I7. It is unlikely that the ethyl group directly adds to the enthalpy of binding the activated OR-I7, since it cannot form hydrogen bonds or engage in other polar non-covalent interactions with the receptor. Nevertheless, the ethyl group triggers activation. One explanation is that the last two carbons of **11**, analogous to those of **C8**, fit into a hydrophobic pocket of the active form where they function as a steric buttress to prevent OR-I7 from reverting to inactive forms (Fig. 7B). This pocket may be closed off in the inactive forms of OR-I7. Since most odorants are hydrophobic, the steric buttress effect may be a general means of stabilizing activated OR forms, as it does not require a polar interaction between the OR and odorant, but can nonetheless generate binding enthalpy by the formation of new intramolecular contacts within the reorganized and activated OR (Kobilka and Deupi, 2007).

Our finding that tightly bent **C8** analogs bind OR-I7 silently suggests that OR-I7 does not use conformational selection to bind only activating conformers of **C8**, but rather that OR-I7 can bind **C8** in many conformations. Proceeding to receptor activation, however, appears to require a double-induced fit, with the agonist unfurling or kinking, as the case may be, to adopt a specific semi-extended conformation that stabilizes the activated form of the receptor. Thus, to be an OR-I7 agonist, an aldehyde must be capable of adopting a conformation in which it can simultaneously plug into two pockets, one specific for the aldehyde functional group and one about 7 Å away having some preference for small hydrophobic rings. The intervening



carbons appear to add binding energy, though to be an agonist C<sub>2</sub>-C<sub>3</sub> must not be substituted when doubly bonded, as previously found (Araneda et al., 2000).

Matching an OR with an activating odorant is the first step toward understanding the structural basis of an OR's contribution to the olfactory code. Once a ligand is identified, rhodopsin based homology modeling can be used to formulate a structural hypothesis for the interaction. Several groups have recently used site-directed mutagenesis within the transmembrane regions to experimentally test predicted odorant-OR interactions (Abaffy et al., 2007; Katada et al., 2005; Schmiedeberg et al., 2007). These studies have obtained experimental support for rhodopsin-based structures, and have generated insightful details into the nature of the OR's binding site. Based on our work, we propose that for ligands with rotatable bonds there will exist conformations favored by the activated and inactive forms of the OR. Experimental evaluation of conformationally restricted odorant analogs may therefore improve homology modeling, since the agonist can be kept in the preferred conformation during the modeling process.

Lastly, we note that it is not yet clear how many ORs are typically activated by a single odorant, though this question is of fundamental importance to understanding the olfactory code. It has been suggested that flexible odorants can activate more ORs than do constrained odorants (Amoore, 1970; Kaluza and Breer, 2000). Our series of eight-carbon aldehydes enabled us to study this question in a controlled manner, and we found that there was indeed a correlation between greater flexibility and the percentage of OSNs activated. Furthermore, we found that a high percentage of C<sub>8</sub>-responding OSNs were activated more potently by conformationally restricted C<sub>8</sub> analogs than by C<sub>8</sub> itself, indicating that many C<sub>8</sub>-detecting ORs, and not just OR-I7, possess some sort of conformational filter. Thus, in analogy to rhodopsin, many ORs appear to be activated or antagonized by specific ligand shapes, even though the ligand may adopt multiple forms (isomers or conformations). The conformationally restricted rings often found in natural fragrance molecules may mimic subsets of conformations in related but more flexible odorants. Some of these mimicked conformers may be high energy and rare, thus contributing to uncommon signatures in the olfactory code.

## SIGNIFICANCE

The molecular recognition of airborne chemicals is challenging because volatility requires low molecular weights and a minimum or absence of polar functional groups, yet this is the subset of chemical space that the olfactory receptors (ORs) have been charged by evolution to monitor. Nearly all odorants have rotatable bonds and can adopt multiple conformations. In a representative system, we have investigated the variable of octanal conformation as a molecular determinant of OR-I7 activation and antagonism. We show that OR-I7 binds a variety of aliphatic aldehydes, but then applies length and conformational criteria that lead either to activation (longer than 6.5-6.9Å) or antagonism (shorter than 6.5-6.9Å). Using a series of octanal mimics, we chart the transition from antagonism to agonism as a function of increasing length. For octanal, the apparent primary agonist for this receptor, we deduce that long and short conformers bind the resting state of OR-I7 and, through a double induced fit, cooperate to produce the activating odorant-OR pair. In mixtures, various OR-I7-bound aldehydes, whether activating or antagonizing, contribute to the olfactory code either positively or negatively, enabling I7 to respond in a gradual manner to mixtures of aliphatic aldehydes rather than to only the best-tuned ligands. By studying nearly 1200 rat olfactory sensory neurons (OSNs), we find evidence that the molecular conformation of flexible odorants appears to be a common determinant of activation, and that fewer OSNs are tuned to rare conformers. For OR-I7, we also find that small cycloalkyl groups at the distal end of an aldehyde enhance activation potency. We propose that they fit into and buttress a small hydrophobic pocket present only in the activated form of the receptor, sterically preventing reversion to the

unactivated form. The steric buttress may be a common strategy for recognizing non-polar odorants, such as the hydrocarbons.

## EXPERIMENTAL PROCEDURES

### Method to estimate the maximum extended length of aldehydes

Chem3D ultra 10.0 software (CambridgeSoft) was used. The structure of the aldehyde was drawn in its most extended conformation. The energy was minimized using the MM2 forcefield. The length was then measured from the carbonyl carbon to the most remote carbon.

### Synthesis of octanal analogs

See Supplemental Data for detailed synthetic procedures and compound characterization.

### Isolation of olfactory sensory neurons (OSNs)

All animal procedures were approved by the Columbia University Institutional Animal Care and Use Committee and performed at Columbia University in compliance with relevant national guidelines and regulations. Procedures for isolating rat OSNs were performed as described in detail elsewhere with minor modifications to the dissociation solution (Araneda et al., 2004). For OR-I7 experiments, male Sprague-Dawley rats 6-7 weeks old were infected with an adenovirus that encoded OR-I7 and GFP as separate proteins (Zhao et al., 1998). 2-3 days following infection, regions of the olfactory epithelium exhibiting dense GFP fluorescence were dissected out. For the panel screening in Fig. 6, uninfected rats were used and the entire olfactory epithelium was collected. The olfactory epithelium was dissected free from the underlying bone under chilled divalent cation-free ringer (mM: 145 NaCl, 5.6 KCl, 10 Hepes, 10 glucose, 4 EGTA, pH 7.4), minced, and then incubated for 45 min in 2.5 mL of divalent cation-free Ringer containing 5 mg/mL bovine serum albumin (Sigma-Aldrich B4287), 1 mg/mL collagenase (Gibco 17100-017), 2.4U/mL dispase II (Roche 04-942-078-001), and 100  $\mu$ L deoxyribonuclease II (Sigma-Aldrich D8764). Following, the tissue was dispersed in a small volume of culture medium (typically 150-200  $\mu$ L) and plated onto concanavalin A coated coverslips. Cells were kept in a 32° C incubator until use.

### Calcium imaging of olfactory sensory neurons

Calcium imaging recordings were performed as described in detail elsewhere (Araneda et al., 2004). Briefly, cells were rinsed with normal rat ringer (mM: 138 NaCl, 5KCl, 1 CaCl<sub>2</sub>, 1.5MgCl<sub>2</sub>, 10 Hepes, 10 glucose, pH 7.4), and loaded with fura-2AM plus pluronic acid for 45 min at room temperature. The coverslip was placed into a recording chamber and imaged at room temperature at 380 nm excitation and 510 nm emission. Due to the slow nature of the calcium response, images were only acquired every 4 sec with each image representing the average of 3 frames. NIH Image software was used for data acquisition and analysis.

Ringer was continuously pumped through the recording chamber at a rate of 1 mL/min. Odorants were presented to the cells by injecting 400  $\mu$ L of the stimulus solution into the chamber over the course of 4 sec, exchanging the volume of the recording chamber 2-3 times. Odorants had been recently synthesized and stored at 4° C under inert atmosphere while awaiting testing. All odorants not specifically synthesized for this study were purchased from Sigma-Aldrich. 0.5M stock solutions of the odorants in DMSO were prepared fresh daily. Stock solutions were subsequently diluted in Ringer to the indicated concentrations with DMSO supplementation as necessary so that all stimuli were matched for the amount of DMSO; cells did not respond to DMSO alone at this level. Odorants were typically applied 3.25 min apart with the exception of the panel screening in Fig.6 where spacing was increased to 5 min apart. Because the cells shown in Fig. 6 all likely express different ORs, the adenylate cyclase

activator forskolin (10  $\mu$ M) was applied at the end of the series to strongly stimulate the downstream signal transduction path and thus provide a means of comparing responses between cells. The response to forskolin also serves as a measure of the functional viability of an OSN since adenylyl cyclase, like the ORs, is localized to the cilia.

Data are shown as the fractional change in fluorescent light intensity,  $(F-F_0)/F_0$ , where  $F$  is the fluorescent light intensity at each point and  $F_0$  is the value for the emitted fluorescent light at the start of each movie before the first stimulus application. Responses were measured between the baseline and peak  $\Delta F/F$  change. To account for drift due to alterations in fluid level or incomplete return of intracellular calcium levels, flanking normalization stimuli (typically C8 or compound **1** at 10  $\mu$ M) were applied at the beginning and end of each movie. A trend line could then be drawn between the peak responses of the flanking applications. Responses to intervening odorants were normalized by taking the ratio of the measured magnitude over the predicted (to trend line) magnitude. Measured in this manner, we found repetitions of the same stimuli meet or exceed 0.90. Accordingly, for the tuning choice in Fig. 6A, we classified two responses as being effectively the same magnitude if they were within 90% of each other, and in Fig. 5D the combination of a putative antagonist with C8 needed to be less than 90% that of C8 alone to be classed as an antagonist. Values for the antagonist ratio reported in Fig. 5D represent the average  $\pm$  SEM. Dose response curves were fit using the Hill function in Igor Pro with each point plotted as the average value from at least three independent GFP-expressing cells  $\pm$  SEM.  $EC_{50}$  and  $IC_{50}$  values are reported as  $\pm$  SD. For marginally activating aldehydes (C6 and compound **4**),  $EC_{50}$  values are extrapolated from the best fit curve.

## Supplementary Material

Refer to Web version on PubMed Central for supplementary material.

## Acknowledgements

This work was funded by the City College of New York Division of Science, the PSC-CUNY and the NIH NIDCD. Additional support was provided by the City College Research Centers in Minority Institutions (RCMI).

## References

- Abaffy T, Malhotra A, Luetje CW. The molecular basis for ligand specificity in a mouse olfactory receptor: a network of functionally important residues. *J Biol Chem* 2007;282:1216–1224. [PubMed: 17114180]
- Amoore, JE. Molecular basis of odour. Springfield, IL: C.C.Thomas; 1970.
- Araneda RC, Kini AD, Firestein S. The molecular receptive range of an odorant receptor. *Nat Neurosci* 2000;3:1248–1255. [PubMed: 11100145]
- Araneda RC, Peterlin Z, Zhang X, Chesler A, Firestein S. A pharmacological profile of the aldehyde receptor repertoire in rat olfactory epithelium. *J Physiol* 2004;555:743–756. [PubMed: 14724183]
- Arctander, S. Perfume and Flavor Materials of Natural Origin. Elizabeth, NJ: Arctander Publishing; 1960.
- Buck L, Axel R. A novel multigene family may encode odorant receptors: a molecular basis for odor recognition. *Cell* 1991;65:175–187. [PubMed: 1840504]
- Chess A, Simon I, Cedar H, Axel R. Allelic inactivation regulates olfactory receptor gene expression. *Cell* 1994;78:823–834. [PubMed: 8087849]
- Dobson CM. Chemical space and biology. *Nature* 2004;432:824–828. [PubMed: 15602547]
- Firestein S. How the olfactory system makes sense of scents. *Nature* 2001;413:211–218. [PubMed: 11557990]
- Firestein S, Picco C, Menini A. The relation between stimulus and response in olfactory receptor cells of the tiger salamander. *J Physiol* 1993;468:1–10. [PubMed: 8254501]

- Gibbs RA, Weinstock GM, Metzker ML, Muzny DM, Sodergren EJ, Scherer S, Scott G, Steffen D, Worley KC, Burch PE, et al. Genome sequence of the Brown Norway rat yields insights into mammalian evolution. *Nature* 2004;428:493–521. [PubMed: 15057822]
- Hall SE, Floriano WB, Vaidehi N, Goddard WA 3rd. Predicted 3-D structures for mouse I7 and rat I7 olfactory receptors and comparison of predicted odor recognition profiles with experiment. *Chem Senses* 2004;29:595–616. [PubMed: 15337685]
- Ho SL, Johnson BA, Chen AL, Leon M. Differential responses to branched and unsaturated aliphatic hydrocarbons in the rat olfactory system. *J Comp Neurol* 2006;499:519–532. [PubMed: 17029262]
- Kaluza JF, Breer H. Responsiveness of olfactory neurons to distinct aliphatic aldehydes. *J Exp Biol* 2000;203:927–933. [PubMed: 10667976]
- Katada S, Hirokawa T, Oka Y, Suwa M, Touhara K. Structural basis for a broad but selective ligand spectrum of a mouse olfactory receptor: mapping the odorant-binding site. *J Neurosci* 2005;25:1806–1815. [PubMed: 15716417]
- Kobilka BK, Deupi X. Conformational complexity of G-protein-coupled receptors. *Trends Pharmacol Sci* 2007;28:397–406. [PubMed: 17629961]
- Krautwurst D, Yau KW, Reed RR. Identification of ligands for olfactory receptors by functional expression of a receptor library. *Cell* 1998;95:917–926. [PubMed: 9875846]
- Ma M, Shepherd GM. Functional mosaic organization of mouse olfactory receptor neurons. *Proc Natl Acad Sci U S A* 2000;97:12869–12874. [PubMed: 11050155]
- Malnic B, Hirono J, Sato T, Buck LB. Combinatorial receptor codes for odors. *Cell* 1999;96:713–723. [PubMed: 10089886]
- Mori K, Nagao H, Yoshihara Y. The olfactory bulb: coding and processing of odor molecule information. *Science* 1999;286:711–715. [PubMed: 10531048]
- Niimura Y, Nei M. Extensive gains and losses of olfactory receptor genes in Mammalian evolution. *PLoS ONE* 2007;2:e708. [PubMed: 17684554]
- Oka Y, Omura M, Kataoka H, Touhara K. Olfactory receptor antagonism between odorants. *Embo J* 2004;23:120–126. [PubMed: 14685265]
- Pilpel Y, Lancet D. The variable and conserved interfaces of modeled olfactory receptor proteins. *Protein Sci* 1999;8:969–977. [PubMed: 10338007]
- Raming K, Krieger J, Strotmann J, Boekhoff I, Kubick S, Baumstark C, Breer H. Cloning and expression of odorant receptors. *Nature* 1993;361:353–356. [PubMed: 7678922]
- Reed RR. After the holy grail: establishing a molecular basis for Mammalian olfaction. *Cell* 2004;116:329–336. [PubMed: 14744441]
- Sakmar TP, Menon ST, Marin EP, Awad ES. Rhodopsin: insights from recent structural studies. *Annu Rev Biophys Biomol Struct* 2002;31:443–484. [PubMed: 11988478]
- Sato T, Hirono J, Tonoike M, Takebayashi M. Tuning specificities to aliphatic odorants in mouse olfactory receptor neurons and their local distribution. *J Neurophysiol* 1994;72:2980–2989. [PubMed: 7897503]
- Schmiedeberg K, Shirokova E, Weber HP, Schilling B, Meyerhof W, Krautwurst D. Structural determinants of odorant recognition by the human olfactory receptors OR1A1 and OR1A2. *J Struct Biol* 2007;159:400–412. [PubMed: 17601748]
- Serizawa S, Miyamichi K, Sakano H. One neuron-one receptor rule in the mouse olfactory system. *Trends Genet* 2004;20:648–653. [PubMed: 15522461]
- Shi L, Javitch JA. The binding site of aminergic G protein-coupled receptors: the transmembrane segments and second extracellular loop. *Annu Rev Pharmacol Toxicol* 2002;42:437–467. [PubMed: 11807179]
- Sicard G, Holley A. Receptor cell responses to odorants: similarities and differences among odorants. *Brain Res* 1984;292:283–296. [PubMed: 6692160]
- Singer MS. Analysis of the molecular basis for octanal interactions in the expressed rat I7 olfactory receptor. *Chem Senses* 2000;25:155–165. [PubMed: 10781022]
- Touhara K. Odor discrimination by G protein-coupled olfactory receptors. *Microsc Res Tech* 2002;58:135–141. [PubMed: 12203691]

- Touhara K, Sengoku S, Inaki K, Tsuboi A, Hirono J, Sato T, Sakano H, Haga T. Functional identification and reconstitution of an odorant receptor in single olfactory neurons. *Proc Natl Acad Sci U S A* 1999;96:4040–4045. [PubMed: 10097159]
- Zhao H, Ivic L, Otaki JM, Hashimoto M, Mikoshiba K, Firestein S. Functional expression of a mammalian odorant receptor. *Science* 1998;279:237–242. [PubMed: 9422698]

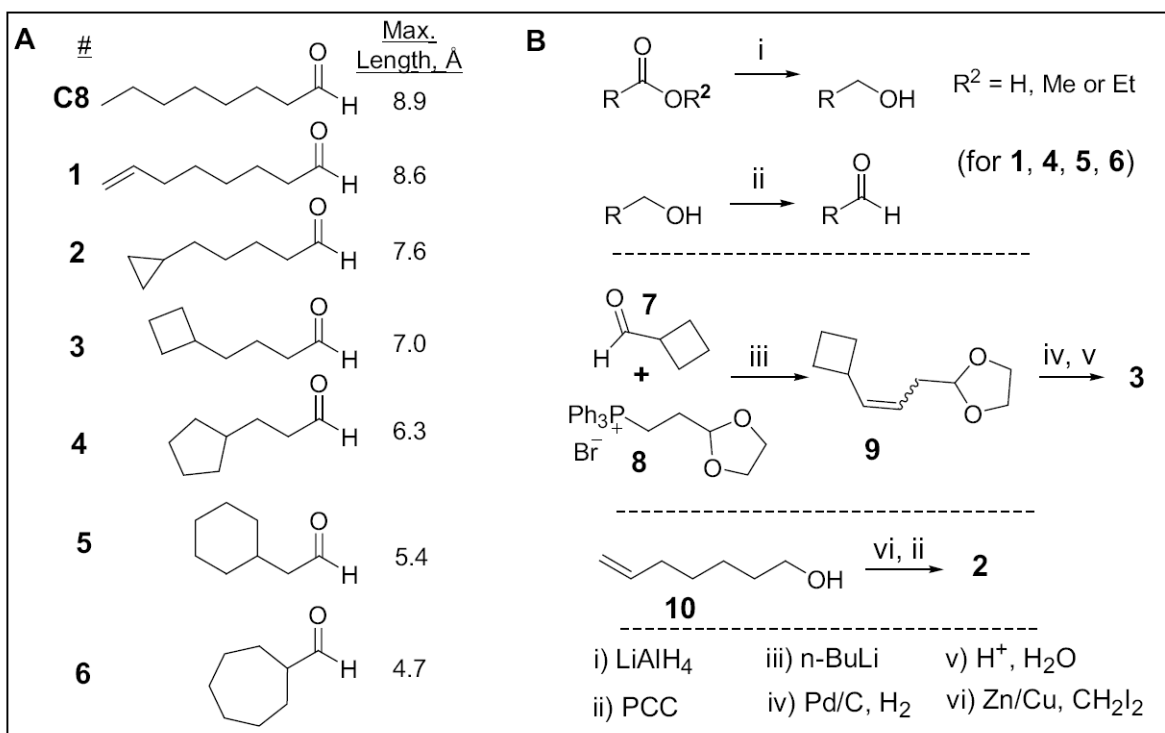


**Figure 1. Conformationally Restricted Octanal Analogs**

(A) Lengths refer to the distance measured from the carbonyl carbon to the most distant carbon as described in Experimental Procedures. (B) Synthetic routes to compounds **1-6**. See Supplemental Data for details.

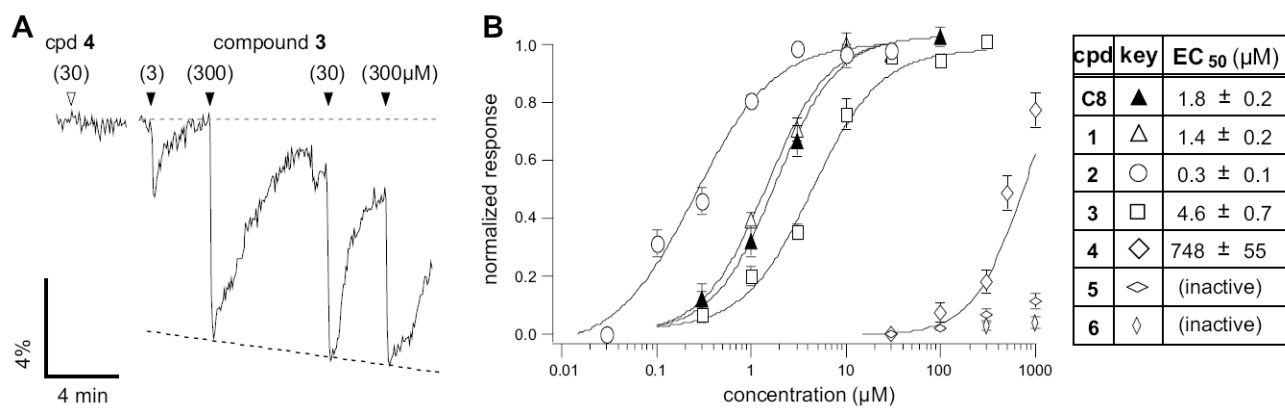


### Figure 2. OR-I7 Activation by Cyclic Octanal Analogs

(A) Calcium imaging traces from a GFP+ OSN, showing how OR-I7 responds at a near saturating level to 30  $\mu$ M of compound **3**, but is unresponsive to compound **4** at the same concentration. Grey dashed line denotes baseline, black dashed line denotes a trend line for normalization (See Experimental Procedures). (B) Activation dose-response curves for the cyclic compound series (open symbols). The activation dose-response curve for octanal (**C8**) is also provided for reference (filled symbol). Octanal and compounds **1-3** saturated over this range and are thus normalized to their respective maximal responses. Compounds **4-6** are shown normalized to the response to 10  $\mu$ M octanal. The maximal efficacies for each compound, relative to 10  $\mu$ M **1**, were as follows (mean  $\pm$  SEM): **2**, 0.99  $\pm$  0.02; **3**, 1.06  $\pm$  0.1; **C8**, 0.89  $\pm$  0.02; **C7**, 0.86  $\pm$  0.07.

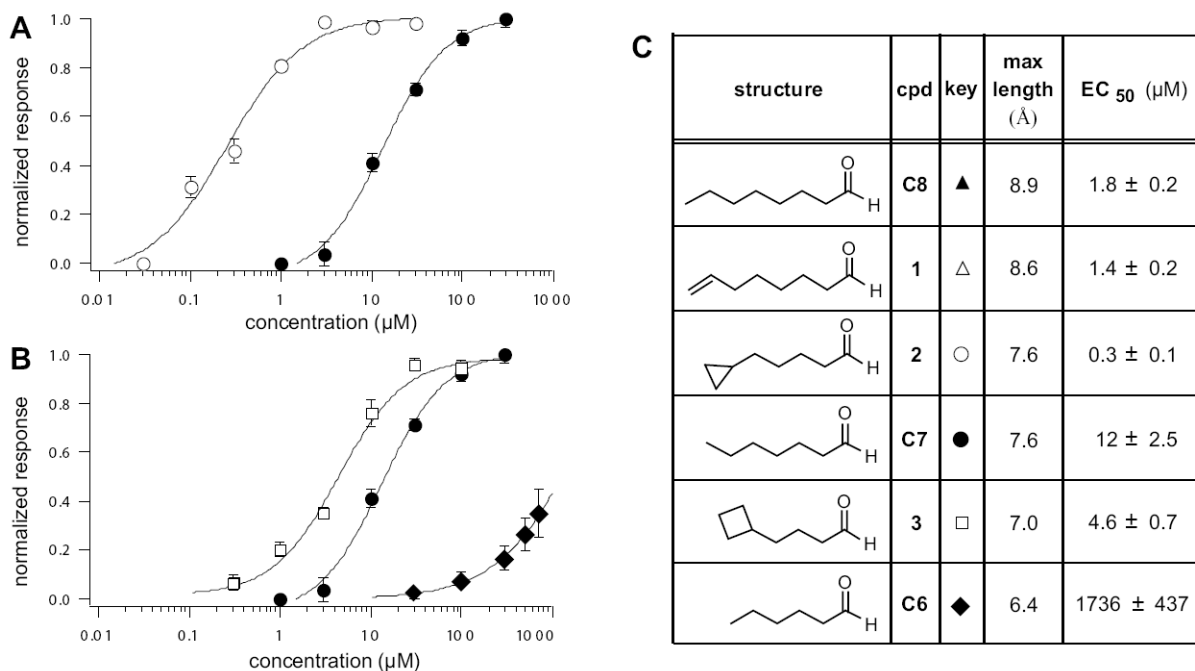


**Figure 3. Cyclopropyl and Cyclobutyl Ring-Containing Analogs Are More Potent Than Predicted from Their Maximal Lengths**

(A) Activation dose-response curves for cyclic compound **2** (open circles) and the n-aldehyde of identical length, **C7** (filled circles). (B) Activation dose-response curves for cyclic compound **3** (open squares) and the n-aldehydes of flanking lengths **C7** (filled circles) and **C6** (filled diamonds). (C) Summary of maximal lengths and  $\text{EC}_{50}$  of activation for the strongly activating cyclic and n-aldehydes. The relative activation of **C8** and compound **1** can be found in Fig. 2B.



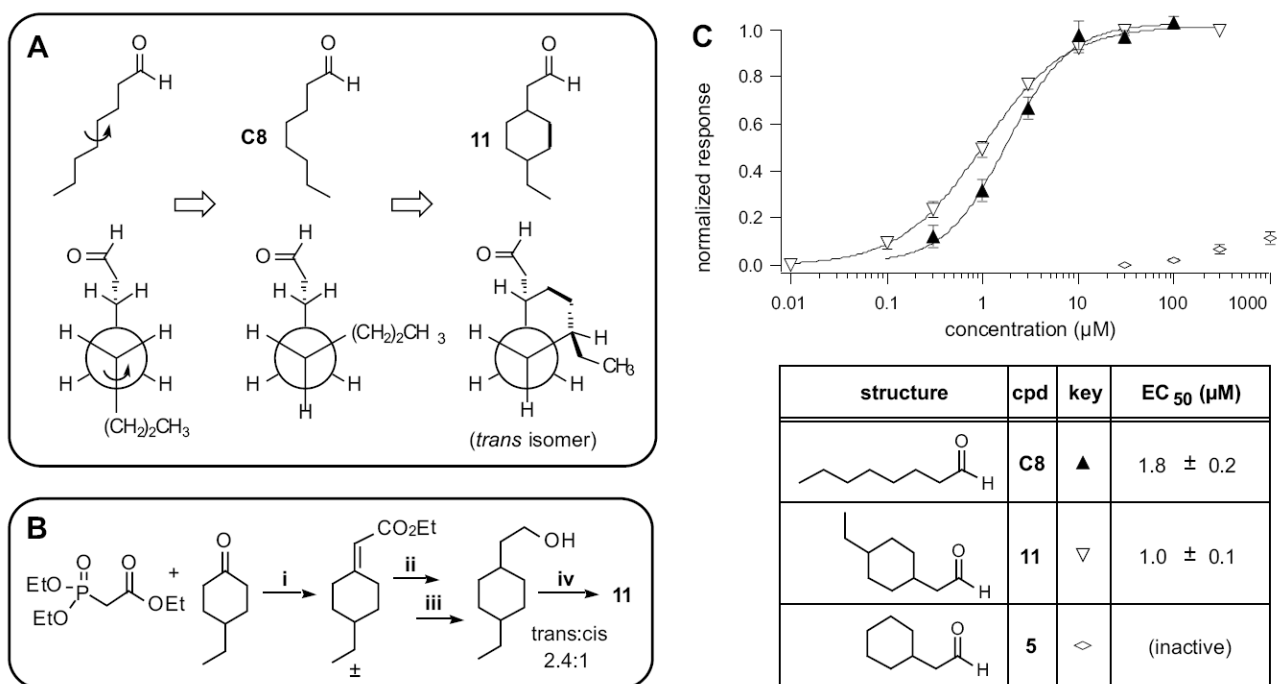


**Figure 4. A Semi-Extended Octanal Conformation Activates OR-I7**

(A) Line structures (top) and Newman projections (bottom) depicting rotation around the C<sub>4</sub>-C<sub>5</sub> bond in octanal, and how it was locked in the gauche conformation in compound **11**. Black dots and arrows denote the extra carbons used to make the conformational lock. Only the trans isomer's Newman projection is shown. (B) Synthetic route to compounds **11**. (C) Activation dose-response curves for octanal (**C8**, filled triangles) and the cis/trans mixture of compound **11** (open inverse triangles). The related compound **5**, which lacks the 4-ethyl group, has no substantial activity (open compressed diamonds). The maximal efficacy for **11** was 1.07 ± 0.05, relative to 10 μM octanal.

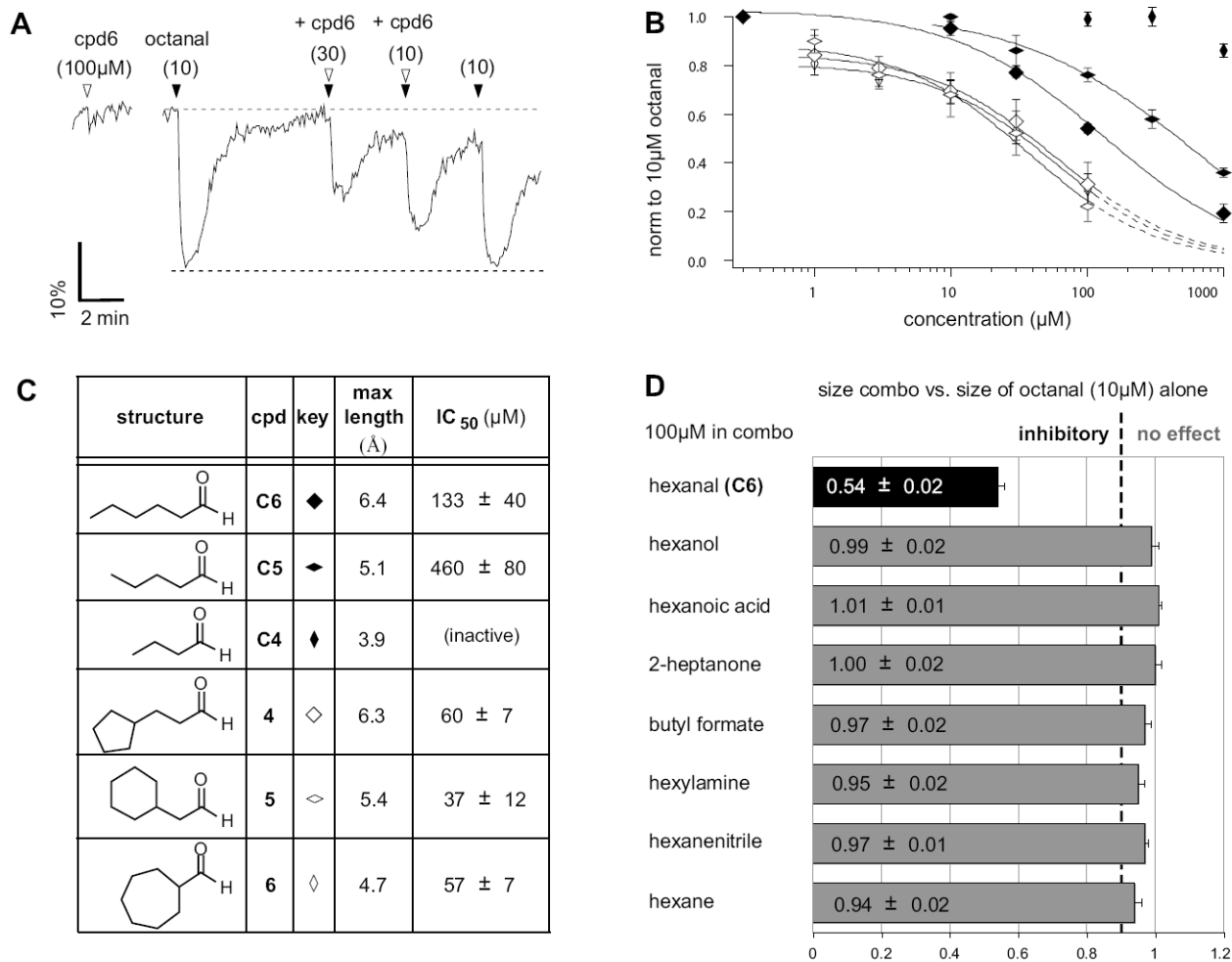


**Figure 5. Inhibition of OR-I7 Activation by Short Octanal Analogs**

(A) Calcium imaging traces from a GFP+ OSN, showing the dose-dependent antagonism of compound **6** against a saturating dose of octanal. Black arrowheads denote the application of 10  $\mu$ M octanal either with or without co-application of **6** (open arrowheads). The black dashed line is the trend line, indicating the predicted response magnitude if the co-application had no effect. (B) Inhibition dose-response curves for cyclic analogs and n-aldehydes of similar lengths, tested at various concentrations against a 10  $\mu$ M octanal stimulus. The cyclic compounds (open symbols) all display very similar potencies regardless of length, while the n-aldehydes (filled symbols) show length dependence for antagonism. Dashed lines indicate extrapolation used to estimate IC<sub>50</sub>. (C) Summary of maximal lengths and IC<sub>50</sub> values for the antagonizing aldehydes. (D) An aldehyde group is required for OR-I7 antagonism. Non-aldehydes of similar size were unable to antagonize octanal activation of OR-I7. Dashed line indicates 90% of the signal produced by 10  $\mu$ M octanal alone.

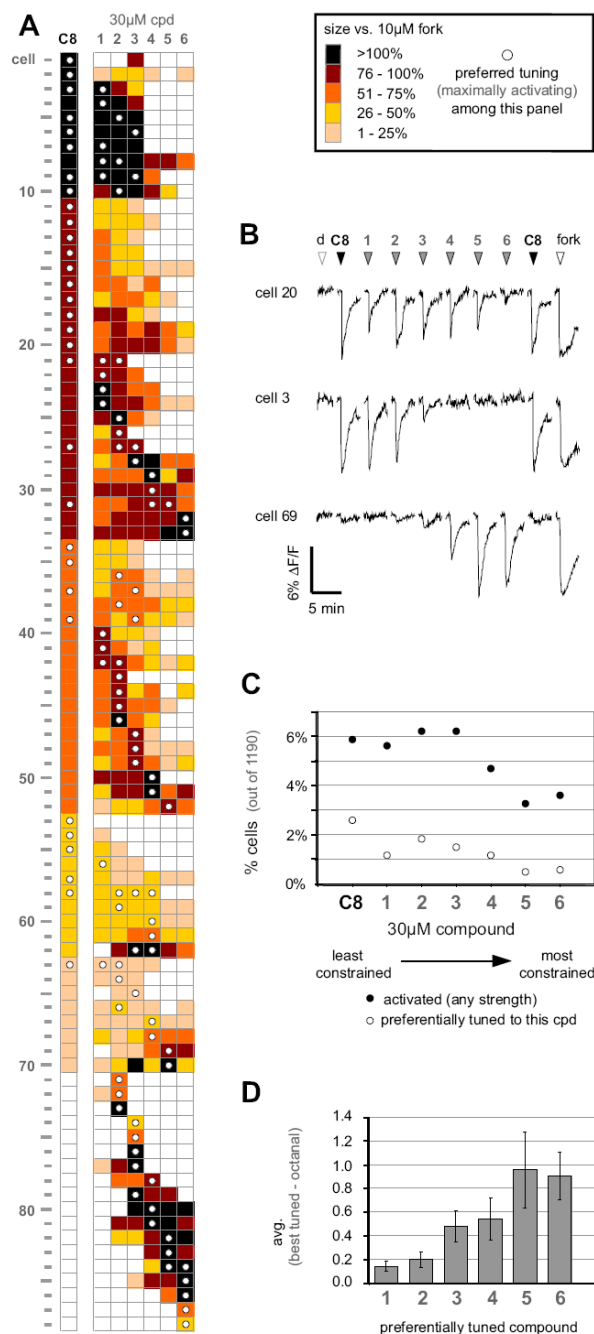


### Figure 6. Conformational Preference Among Octanal Receptors

(A) Response profiles of the entire population of OSNs activated by 30  $\mu$ M octanal (C8) or the cyclic analogs 1-6 out of 1190 tested OSNs. Only responding cells are represented. Response strength was normalized within each cell to 10  $\mu$ M of the adenylate cyclase activator, forskolin, to gauge near maximal activation of the signal transduction cascade. The compound eliciting the greatest response by the cell (i.e. its preferred tuning) is denoted by a white dot. (B) Representative calcium-imaging traces from three selected cells exposed to aldehydes 1-6, each given individually at 30  $\mu$ M. Compounds were tested in random order, but have been rearranged for presentation clarity. The open arrowheads denote application of the DMSO vehicle (d) or forskolin (fork). (C) Percentages of OSNs responding to 30  $\mu$ M of the indicated

compound among the 1190 tested cells (filled circles) and percentages of cells preferentially tuned to the indicated compounds (open circles). (D) Average difference in activation strength between analogs and octanal. For the cells whose preferred tuning included a cyclic analog, the response to octanal was subtracted from the response to the preferred analog. This difference was then averaged over all cells tuned to that same analog. Because all responses are normalized within each cell to forskolin activation, the maximum possible difference is 1.0 (i.e. the case where a cell responds as robustly to the preferred analog as forskolin but fails entirely to respond to octanal).

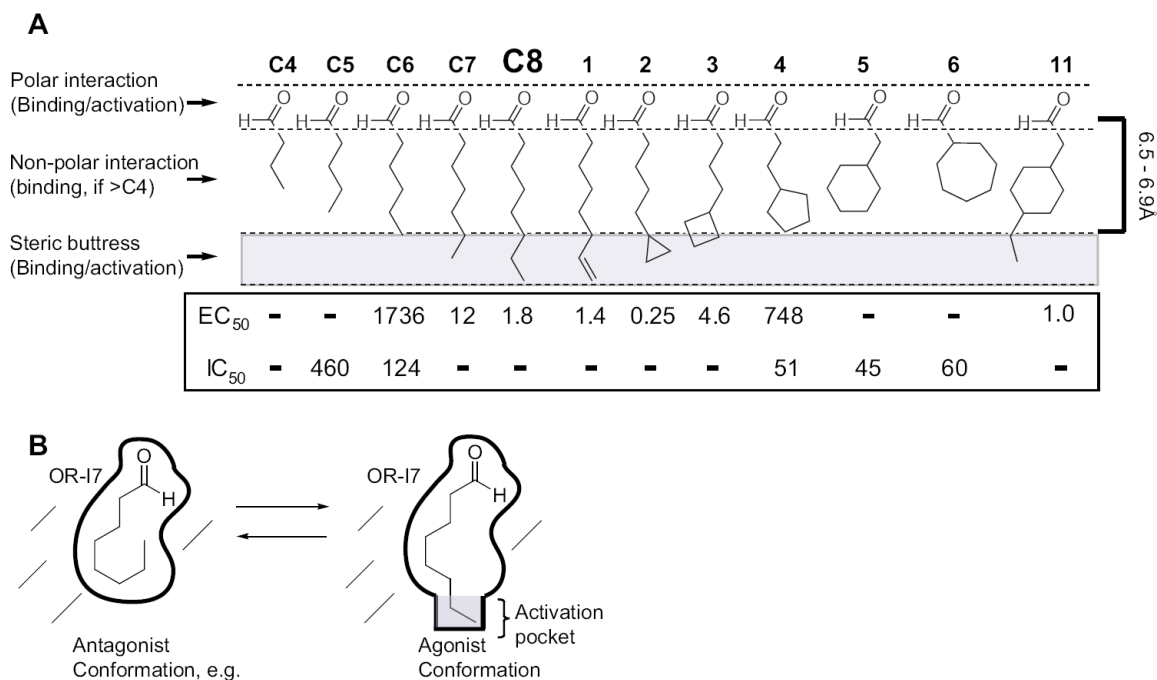


**Figure 7. Summary of OR-17 binding and activation by octanal conformation mimics**

(A) Structures, maximum lengths, and inhibition/activation constants. Regions of the structures responsible for binding and activation are indicated (left), as is the 6.5-6.9Å length requirement for activation (right). Except for C4, which had neither type of activity, dashes in the IC<sub>50</sub> row indicate that the compound was not tested for antagonism because it is strongly activating. Dashes in EC<sub>50</sub> row indicate the compound had no activity within its solubility range. (B) Schematic depiction of octanal's conformation on OR-17's activation.